Record of Jurassic mass transport processes through the orogenic cycle: Understanding chaotic rock units in the high-pressure Zermatt-Saas ophiolite (Western Alps)

Abstract (max. 200 parole)

The eclogite-facies Zermatt-Saas ophiolite in the western Alps includes a composite chaotic unit exposed in the Lake Miserin area located in the southern Aosta Valley region. The chaotic unit is characterized by a block-in-matrix texture consisting of mafic/ultramafic clasts and blocks embedded within a carbonate-rich matrix. This unit overlies massive serpentinite and ophicarbonate rocks and is unconformably overlain by layered carbonate-rich calcschists. Despite the effects of subduction and collision-related deformation and metamorphism, the internal stratigraphy and architecture of the chaotic unit is recognizable and attributed to mass transport processes, actingin the Jurassic Ligurian - Piedmont Ocean. This finding represents an exceptional record of the pre-orogenic history of the Alpine ophiolites marked by different pulses of extensional tectonics responsible of the rough seafloor topography characterized by structural highs exposed to submarine erosion. The Jurassic tectono-stratigraphic setting here envisioned is closely comparable with that observed in present-day “magma-poor” slow- and ultraslow-spreading ridges characterized by mantle exposure along fault scarps which trigger mass transport deposits and turbiditic sedimentation. Our pre-orogenic reconstruction is significant in an eclogitized collisional orogenic belt in which, chaotic rock units may be confused with the exclusive product of subduction-related tectonics, deleting the record of an important pre-orogenic history.

Key words: Western Alps; ophiolite; syn-extension and post-extension sedimentary sequences, mélanges and broken formations; mass transport deposits.

INTRODUCTION

Jurassic Tethyan ophiolites emplaced in the Alpine orogen widely contributed to the discussion on the ophiolite concept (see Lagabrielle, 2009 for a review). Although, in the last two decades, the attention on Alpine ophiolites was mainly focused on the definition of their subduction- and collision-related P-T-t trajectories, multidisciplinary field studies demonstrated that those ophiolite may preserve meaningful records of the pre-Alpine ocean-related history (e.g., Balestro et al., 2015a; Festa et al., 2015), allowing to reconstruct the Jurassic tectonostratigraphic architecture, which is comparable with that observed in present-day “magma-poor” slow- and ultraslow-spreading ridges (e.g., Mével et al., 1991; Dick et al., 2003; Boschi et al., 2006; Escartin et al., 2008).

In this paper, we document the internal architecture of the Lake Miserin Ophiolite (LMO hereafter), which is part of the eclogite-facies Zermatt-Saas ophiolite (Western Alps). Detailed stratigraphic and structural analysis of different block-in-matrix structures occurring in a composite chaotic unit, allowed us documenting that, despite the overprint of subduction and collision-related deformation, exceptional records of intra-oceanic tectono-sedimentary processes are preserved as the product of tectonically induced mass transport processes, which acted along the flanks of a mantle structural high in the Jurassic Ligurian - Piedmont Ocean (JLPO herefater). The Jurassic tectono-stratigraphic setting which we reconstruct is closely comparable with those observed in present-day “magma-poor” slow- and ultraslow-spreading ridges (e.g., Mével et al., 1991; Cannat, 1993; Dick et al., 2003; Boschi et al., 2006), providing profound implications in interpreting the primary physiography and paleo-topography of the JLPO seafloor and in better understanding present-day oceanic settings.

REGIONAL GEOLOGY

The Zermatt-Saas ophiolites (Bearth, 1967; see Martin et al., 1994 for a review) emplaced during the closure of a branch of the Jurassic Tethyan ocean (i.e., the JLPO), interposed between the European and African plates. They are tectonically stacked in the axial sector of the Western Alps (i.e. the Piedmont Zone; see e.g. Dal Piaz et al., 2003), resulting from deformation and metamorphism occurred during (i) Late Cretaceous to Middle Eocene SE-dipping subduction, (ii) Late Eocene–Early Oligocene collision and NW-verging accretion, and (iii) Oligocene to Neogene exhumation.

The LMO crops out in the southern sector of the Mount Avic ultramafic massif (Fig. 1). The latter shows an early Alpine metamorphic overprint under eclogite-facies conditions, partially re-equilibrated under blueschists- to greenschists-facies conditions (e.g., Dal Piaz et al., 2010), and consists of serpentinized metaperidotite intruded by Fe-Ti- and Mg-metagabbros, which are covered by different metasedimentary successions (Fontana et al., 2008; Panseri et al., 2008). The northern sector of the Mount Avic ultramafic massif is particularly characterized by the occurrence of (*i*) mafic/ultramafic metabreccia and meta-ophicalcite (Tartarotti et al., 1998; Dresnier, 1993), documenting mantle sea-floor exhumation, and (*ii*) Mn ore deposits and Fe-Cu sulphide mineralizations. The latters were attributed to original hydrothermal vents (i.e. black smokers; Martin et al., 2008; Tumiati et al., 2010), highlighting that mantle rocks were exhumed close to a ridge center.

THE LAKE MISERIN OPHIOLITE (LMO)

The LMO consists of serpentinite followed, through a meta-ophicalcite horizon, by a Composite Chaotic Unit (CCU hereafter) made of serpentinite blocks and disrupted metasandstone and metabreccia horizons of ultramafic composition, embedded within a carbonate-rich matrix. A Calcschist Unit directly overlies either the CCU, or the serpentinite and meta-ophicalcite (Figs. 2A-C).

The serpentinite derives from peridotite of likely lherzolite composition. It consists of antigorite with mesh texture, Ti-clinohumite, oxides (Cr-Ni-rich magnetite, ilmenite, and chromite with Cr# ranging between 60 and 80), and clinopyroxene with both magmatic augite (En_{47-49}, Wo_{48-50}, Fs_{1-2}) and metamorphic diopside/wollastonite ($En_{45-48,}$ Wo_{49-51}, Fs_{1-3}) compositions. Upwards, the serpentinite contains crosscutting sets of veins, up to 1-2 cm thick and filled with carbonate, antigorite, or talc, which bound decimeter- to meter-sized "clasts" of massive serpentinite. Veined serpentinite are covered by a meta-ophicalcite horizon (Fig. 3A), up to one meter thick and both are characterized by the occurrence of carbonate-rich nodules with a typical orange colored alteration coating.

The LMO was deformed during at least three superposed Alpine-related deformation phases (named D1, D2 and D3). D1 is coeval to the subduction-related eclogite-facies metamorphism, and developed the S1 foliation, which is parallel to the lithological contacts and overprinted the primary surfaces (i.e., the S0 sedimentary bedding). D2 is coeval to the collision-related blueschists- to greenschists-facies re-equilibration, and is characterized by N-S trending isoclinal folds (Fig. 2D) which pervasively deform the meta-ophiolite succession. D2 folds developed a W-NW-dipping axial plane foliation (i.e. the S2) and are characterized by boudinage along long fold limbs. D3 is coeval to the exhumation stage and is characterized by NW-SE trending gentle folds (Fig. 3E) which deform the previous D1+D2 structural architecture.

The Composite Chaotic Unit (CCU)

The CCU corresponds to a wedge shaped unit in cross-section, which increases in thickness from zero to about 40 meters from WSW to ENE and N (Fig. 2), showing lateral and vertical change of facies of its block-in-matrix fabric. It consists of three types of broken formation (*sensu* Hsü, 1968), i.e., BrFm1, BrFm2 and BrFm3, and a sedimentary mélange (*sensu* Raymond, 1984 and Festa et al., 2012), i.e., SedMé. The contact between the different types of chaotic rock units is transitional and it does not show any traces of Alpine-related mylonitic deformation.

Type 1 Broken Formation (BrFm1)

The BrFm1 consists of different superposed bodies of ultramafic metabreccia, ranging in thickness from 1 to 3 m (Figs. 2F-G), and characterized by an internal normal grading. Metabreccia varies from clast- to matrix supported, with irregular to sub-rounded shaped clasts ranging in size from decimeters to centimeters (Fig. 3B). The matrix consists of a coarse-grained metasandstone of the same composition of clasts. Rare elongated blocks, up to 50 cm long, are randomly distributed within the metabreccia. The BrFm1 shows a lenticular shape at scale of hundreds of meters with a maximum thickness of about 15 m (Figs. 2F-G). The contact with serpentinite is sharp, locally corresponding to a decimeters thick layer of coarse -to medium-grained metasandstone of ultramafic composition.

Type 2 Broken Formation (BrFm2)

The BrFm2 consists of disrupted horizons, decimeters in thickness, of clast-to matrix supported metabreccia and coarse-grained metasandstone embedded in a carbonate-rich matrix (Fig. 3C), which gradually passes upward from calcschist to whitish marble. It crops out in the eastern and northeastern sectors of the studied area, showing a wedge-like shape varying from zero to about 15 m in thickness from SSW to NNE (Figs. 2F-G), and resting directly onto the meta-ophicalcite horizon through a sharp contact marked by a centimeters-thick calcschist horizon. Disrupted horizons of detrital ultramafic metabreccia are prevalent in the basal part, and show an internal normal grading marked by angular to irregular shaped clasts, up to centimeters in size, passing upward to metasandstone. Those horizons are boudinated at meters scale as a result of D2 deformation (Fig. 3C). The marble matrix prevails in the upper part, showing a transitional contact with the above SedMé unit.

Sedimentary mélange (SedMé)

The SedMè is characterized by a block-in-matrix fabric (Figs. 3D-E) with mainly rounded to irregular and equiangular exotic blocks of massive to veined-serpentinite and meta-ophicalcite, decimeters to one meter in size, embedded within a whitish marble matrix. Carbonate veins, decimeters long and up to 1-2 cm thick, are bounded within the blocks and does not cross the

matrix (Fig. 3E). Blocks are randomly distributed within the matrix (see Figs. 3D-E) and only rare elongated shaped blocks are aligned to the S2 foliation. The matrix commonly includes centimeters-thick horizons of metabreccia of ultramafic composition, which are characterized by angular or sub-angular clasts of serpentinite (Fig. 3F). The entire detrital horizons are foliated (S1-S2) and folded (D2), constraining the brecciation process as having occurred before the D1 deformation stage (i.e., before the subduction-related deformation stage; Fig. 3G). In the upper part of the unit, blocks decrease in size (i.e., up to decimeters) and the matrix is gradually interfingered by centimeters thick levels of calcschist, which marks the transition to the above BrFm3. The SedMé shows a wedge-like shaped geometry ranging in thickness from few meters to 15-20 meters, from SW to NE (Figs. 2F-G). In the southwestern sector, it directly overlies the massive serpentinite and the meta-ophicalcite.

Type 3 Broken Formation (BrFm3)

The BrFm3 represents the uppermost part of the CCU. It shows similar characteristics to BrFm2, consisting of a calcschist and marble matrix, embedding disrupted horizons and bed fragments, decimeters to meters long and up to decimeters thick, of medium-grained metasandstone of ultramafic composition (Fig. 3H). The elongated to sigmoidal shape of blocks, is consistent with D2-related boudinage. This unit, which shows an average thickness of about 10 m, decreases in thickness toward WNW where it directly overlies the BrFm1 and it is followed upward by the Calcschist Unit (Figs. 2F-G).

Calcschist Unit

The CCU and underlying massive serpentinite are unconformably overlain by layered carbonate-rich calcschist (Fig. 2), devoid of any ophiolite-derived detrital material, and alternating with levels of quartz-rich schist. The basal contact between this succession and the underlying lithostratrigraphic units is sharp and corresponds to a depositional surface as inferred form the lack of any mylonitic structure associated with it (Fig. 3I). The unconformable contact at the base of

calcschist is folded together with the units below due to the superposition of D2- and D3-related folding (Fig. 2B).

THE LAKE MISERIN OPHIOLITE AS A PRODUCT OF JURASSIC MASS TRANSPORT PROCESSES

We interpret the LMO as a remnant of an intra-oceanic structural high of the JLPO lithosphere and the CCU as the product of downslope mass transport processes related to Jurassic extensional tectonics. By unravelling the Alpine deformation in the CCU, it is possible to understand its significance in the context of extensional tectonics leading to mantle exhumation in the JLPO. The chaotic block-in-matrix arrangement of BrFm2 and BrFm3, is related to the tectonic dismemberment of their primary stratigraphic organization by means of the D1- and D2 Alpine deformation, whereas the BrFm1 and SedMé fabric was acquired by mass-transport processes acted at the time of Jurassic extensional tectonics.

The BrFm2 and BrFm3 consist of calcschist with disrupted horizons of metasandstone and metabreccia of ultramafic composition which represent native components (i.e., turbiditic horizons) with respect to the carbonate-rich matrix (e.g., Balestro et al., 2015b). The BrFm1, which consists of blocks and matrix of the same composition, corresponds to a “serpentinite matrix broken formation”, being composed of only native components, but showing strong analogies with “serpentinite matrix mélanges” described in the Franciscan Complex and US-Western Cordillera (e.g., Wakabayashi, 2015 and reference therein). The block-in-matrix arrangement of the SedMé represents the emplacement of exotic components with respect to the carbonate matrix. The random distribution of blocks suggests an original emplacement through gravitational processes (see below), rather than tectonic slicing. The occurrence of carbonatic veins, which are bounded within the same blocks, also constrains their exotic nature, sourced from the primary ophicalcite horizon.

The Composite Chaotic Unit: a record of tectono-sedimentary processes

The wedge-shaped architecture of the CCU, its internal fabric and subdivision, and the nature of the contacts with the underlying serpentinite suggest tectonically induced mass transport sedimentation spatially and temporally associated with extensional deformation and erosion along an intra-oceanic bathymetric high (Figs. 4A-D). The vertical and lateral organization of the BrFm2, which consists of a wedge-shaped fining-upward succession of alternating metabreccia/metasandstone horizons of ultramafic composition and calcschist passing upward to marble, represents the deposition of channelized turbidites. The prevalent occurrence of brecciated horizons alternating with calcschist in the lower part of this succession suggests proximal deposition close to a submarine escarpment with high depositional energy, recording a first extensional stage of mantle denudation (Fig. 4A). The upward gradual increasing of the carbonate component within the matrix and decreasing of grain size within the ultramafic detrital horizons, are consistent with the progressive decrease of depositional energy, suggesting in turn a decrease of tectonic activity and/or deepening of the relative sea level.

The block-in-matrix arrangement of the SedMé, with serpentinite blocks embedded within a carbonate matrix, records a new significant pulse of extensional tectonics (Fig. 4B). The random distribution of blocks within the matrix and the occurrence of carbonate veins confined only within the blocks, suggests their collapse from bathymetric/structural highs exposing both serpentinized peridotite and ophicalcite. The upward decrease of blocks size up to the gradual transition to BrFm3, is consistent with the gruadual decrease in magnitude of this tectonic activity. BrFm3 records a new turbititic input (Fig. 4C). Its direct superposition onto the BrFm1 (Fig. 3B) and locally onto the serpentinite suggests that the BrFm1 was originally located on a topographic high mainly consisting of mantle rocks exposed to *in situ* mechanical fracturing and erosion, thus representing part of the source area for the ultramafic detrital components interfingered within the CCU (Figs. 4B-C).

The wedge shape of the CCU, which thickens toward ENE, is consistent with the vertical change of facies of each single unit and with a paleo-escarpment probably dipping toward the same direction (at present-day coordinates).

The unconformable deposition of the Calscschist Unit (Fig. 4D), overlying both the CCU and the serpentinite, represents a post-extensional succession that was deformed and folded during Alpine tectonic stages, together with the underlying sequence. Ophiolitic-detrital material is lacking and the occurrence of quartz-rich schist records an input of continental-derived sediments within the basin, which is thus filled by distal mixed siliciclastic-carbonatic turbidites reworking a passive margin source area. This depositional stage, which coincides with significant terrigenous input into the basin, is well comparable with Early Cretaceous post-extensional deposits preserved in the unmetamorphosed Ligurian Units in the Northern Apennines (e.g., Decandia and Elter, 1972).

The Lake Miserin ophiolite and the physiography of the Jurassic Ligurian – Piedmont seafloor

Pre-orogenic reconstruction of the LMO implies tectonic denudation of mantle rocks at the seafloor of the JLPO, as it has been widely documented in modern slow- and ultraslow-spreading ridges (e.g., Mével et al., 1991; Dick et al., 2003; Escartin et al., 2008). Meta-ophicalcite records the early history of lithospheric mantle exumation by extensional tectonics, and of concurrent hydrothermal fluids circulation on the JLPO seafloor. Brecciation and mass transport deposits recorded in the CCU are evidence of tectonically-induced sedimentation during the mature stage of ocean opening, thus representing syn-extensional (i.e., syn-rift) deposits. Similar serpentinite breccias have been observed in serpentinite bodies of the Atlantic ocean exposed along the western median valley wall of the MARK (Mid Atlantic Ridge-Kane fracture zone) area. Submersible diving on *Alvin* (Karson et al., 1987) and *Nautile* (Mével et al., 1991) reveal that this region is characterized by active faulting and mass wasting dominated by extensive debris slide deposits (see also Karson and Lawrence, 1997): along steep fault scarps foliated serpentinites are directly overlain by coarse, clast-supported breccia consisting of angular cobbles of foliated serpentinite in a matrix of consolidated carbonate. Furthermore, in the median valley wall of the MARK area, mass transport processes has produced rock deposits with angular shapes, similar to those found in our broken formations. In our model, the serpentinite breccia of BrFm1 could have been reactivated by normal faults (as suggested for the MARK area; see Karson and Lawrence,

1997) providing the source material delivered to breccia of BrFm2, BrFm3 and SedMé.

The recognition, for the first time in this sector of the Western Alps of the unconformable deposition of the post-extensional Calcschist Unit, sealing the syn-extensional LMO architecture, is well comparable with the Valanginian–early Aptian post-rift siliciclastic rocks interfingering with carbonate-rich turbiditic deposits in the Deep Galicia margin (Winterer et al., 1988), which represents an excellent modern analogue for the post-extensional succession that we describe from the LMO. The close similarity with the Early Cretaceous post-extensional calcschist in other Alpine (Festa et al., 2015) and Northern Apennines (e.g., Decandia and Elter, 1972) ophiolites, marks the critical timing of the final opening stages of the JLPO.

Our results have thus profound implications for the physiography and geodynamics of the JLPO: the occurrence of pre-orogenic, syn-extensional deposits indicate that the seafloor of the JLPO should have been characterized by regions of active faulting responsible for the formation of a rugged seafloor topography exposed to widespread gravitational processes (Fig. 4E. Furthermore, the occurrence of paleo-hydrothermal vents in the ultramafic massif (i.e. the Mount Avic) which includes the LMO, highlights that mantle rocks were exhumed close to a ridge center (Fig. 4E).

CONCLUSIONS

Our findings document, in the eclogitized Zermatt-Saas ophiolite, exceptionally preserved records of mass transport deposits and turbiditic sedimentation, which formed by intra-oceanic tectono-sedimentary processes during the Late Jurassic syn-rift stages of the Ligurian – Piedmont oceanic basin. The understanding of the meaning of each type of chaotic rock unit within the LMO allowed us to detail the role played by different pulses of extensional tectonics associated with mantle exhumation and their control of sedimentation. This is significant to be reconstructed in an eclogitized collisional orogenic belt in which, the occurrence of chaotic rock units may be commonly confused and interpreted as the exclusive product of subduction-related tectonics, deleting the record of an important pre-orogenic history. Significant for our interpretation resulted

274 the detailed analysis of block-in-matrix structures in the CCU, which allowed unraveling Alpine
275 deformation and reconstructing pre-Alpine history.
276
277
278 **REFERENCES**

279 Balestro, G., Festa, A., Dilek, Y., and Tartarotti, P., 2015a, Pre-Alpine extensional tectonics of a
280 peridotite-localized oceanic core complex in the Late Jurassic, high-pressure Monviso.
281 Episodes, v.38(4), p.266-282.
282 Balestro, G., Festa, A., and Tartarotti, P., 2015b, Tectonic significance of different block-in-matrix
283 structures in exhumed convergent plate margins: Examples from oceanic and continental
284 HP rocks in inner western Alps (northwest Italy): International Geology Review, v.57(5–8),
285 p.581–605.
286 Boschi, C., Früh-Green, G.L., and Delacour, A., 2006, Mass transfer and fluid flow during
287 detachment faulting and development of an oceanic core complex, Atlantis Massif (MAR
288 30°N): Geochemistry, Gephysics, Geosystem, v.7, doi: 10.1029/2005GC001074.
289 Bearth, P., 1967, Die Ophiolithe der Zone von Zermatt-Saas Fee. Beiträge zur Geologischen Karte
290 der Schweiz, Neue Folge, 132, 130 pp.
291 Dal Piaz, G.V., Bistacchi, A., and Massironi, M., 2003, Geological outline of the Alps: Episodes,
292 v.26, p.175–180.
293 Dal Piaz, G.V., Pennacchioni, G., Tartarotti, P., Carraro, F, Gianotti, F., Monopoli, B., G., Schiavo,
294 A., 2010, Carta Geologica d'Italia alla scala 1:50.000, Foglio 091 "Chatillon" con Note
295 Illustrative, Ed. ISPRA.
296 Decandia, F.A., and Elter, P., 1972, La "zona" ofiolitifera del Bracco nel settore compreso fra
297 Levanto e la Val Graveglia (Appennino Ligure): Memorie della Societa Geologica Italiana,
298 XI, p.503–530.
299 Dick, H.J.B., Lin, J., and Schouten, H., 2003, An ultraslow-spreading class of ocean ridge: Nature,
300 v. 426, p.405-412.

301 Driesner, T., 1993, Aspects of petrographical, structural and stable isotope geochemical evolution
302 of ophicarbonate breccias from ocean floor to subduction and uplift; an example from
303 Chatillon, Middle Aosta Valley, Italian Alps: Schweiz. Mineral. Petrogr. Mitt., v.73(1), p.69-
304 84.
305 Escartin, J., and Canales, J.P., 2011, Detachments in oceanic lithosphere: Deformation,
306 magmatism, fluid flow and ecosystems: Eos, Transactions, American Geophysical Union,
307 v.92, pp.31.
308 Escartin, J., Smith, D.K, Cann, J., Schouten, H., Langmuir, C.H., and Escrig, S., 2008, Central role
309 of detachment faults in accretion of slow-spreading oceanic lithosphere: Nature, v.455,
310 doi: 10.1038/nature07333.
311 Festa, A., Dilek, Y., Pini, G.A., Codegone, G., and Ogata, K., 2012, Mechanisms and processes of
312 stratal disruption and mixing in the development of mélange and broken formations:
313 Refining and classifying mélanges: Tectonophysics, v.568-569, p.7-24.
314 Festa, A., Balestro, G., Dilek, Y., and Tartarotti, P., 2015, A Jurassic oceanic core complex in the
315 high-pressure Monviso ophiolite (western Alps, NW Italy): Lithosphere, v. 7, p.646-652.
316 Fontana, E., Panseri, M., and Tartarotti, P., 2008, Oceanic relict textures in the Mount Avic
317 serpentinites, Western Alps: Ofioliti, v. 33(2), p.105-118.
318 Hsü, K. J., 1974, Melanges and their distinction from olistostromes: SEPM Spec. Publ., v.19, p.
319 321-333.
320 Karson, J.A., Thompson, G., Humphris, S.E., Edmond, J.M., Bryan, W.B., Brown, J.R., Winters,
321 A.T., Pockalny, R.A., Campbell, A.C., Klinkhammer, G., Palmer, M.R., Kinzler, R.J., and
322 Sulanowska, M.M., 1987, Along axis variations in seafloor spreading in the MARK area:
323 Nature, v.328, p.681-685.
324 Karson, J.A. and Lawrence, R. M., 1997, Tectonic setting of serpentinite exposures on the
325 Western median valley wall of the MARK area in the vicinity of Site 920, In: Karson, J.A.,
326 Cannat, M., Miller, D.J., and Elthon, D. (Eds.), Proceedings of the Ocean Drilling Program,
327 Scientific Results, v.153, p.5-21.
328 Lagabrielle, Y., 2009, Mantle exhumation and lithosphere spreading: An historical perspective from

329 investigations in the oceans and in the Alps-Apennines ophiolites: Italian Journal of
330 Geosciences, v.128 (2), p.279-293.
331 Martin, S., Tartarotti, P., and Dal Piaz, G.V., 1994, The Mesozoic ophiolites of the Alps: a review:
332 Boll. Geofisica Teoria e Applicata, v.36, p.175-219.
333 Martin, S., Rebay, G., Kienast, J.-R., and Mével, C., 2008, An eclogitised oceanic palaeo-
334 hydrothermal field from the St. Marcel valley (Italian Western Alps): Ofioliti, v.33(1), p.49-
335 63.
336 Mével, C., Cannat, M., Gente, P., Marion, E., Auzende, J.-M. and Karson, J.A., 1991,
337 Emplacement of deep crustal and mantle rocks on the west median valley wall of the
338 MARL area (MAR, 23°N): Tectonophysics, v.190, p.31-53.
339 Panseri, M., Fontana, E., and Tartarotti, P., 2008, Evolution of rodingitic dykes: metasomatism and
340 metamorphism in the Mount Avic serpentinites (Alpine ophiolites, southern Aosta valley):
341 Ofioliti, v.33 (2), p.165-185.
342 Raymond, L.A., 1984, Classification of melanges, Geol. Soc. Am. Special Paper n. 198, p. 7-20..
343 Tartarotti, P., Benciolini, L., and Monopoli, B., 1998, Brecce serpentinitiche nel massiccio
344 ultrabasico del Monte Avic (Falda Ofiolitica Piemontese): possibile evidenze di erosione
345 sottomarina: Atti Tic. Sc. Terra, v.7, p.73-86.
346 Tumiati, S., Martin, S., Godard, G., 2010, Hydrothermal origin of manganese in the high-pressure
347 ophiolite metasediments of Praborna ore deposit (Aosta Valley, Western Alps). European
348 Journal of Mineralogy, v.22, p.577–594
349 Wakabayashi, J., 2015, Anatomy of a subduction complex: architecture of the Franciscan
350 Complex, California, at multiple length and time scales: International Geology Review,
351 v.57, p.669-743.
352 Winterer, E.L., Gee, J.S., and Van Waasbergen, R.J., 1988, The source area for Lower
353 Cretaceous clastic sediments of the Galicia Margin: geology and tectonic and erosional
354 history, *in* Boillot, G., Winterer, E.L., et al., Proc. ODP, Scientific Results, v.103: College
355 Station, TX (Ocean Drilling Pro-gram), p.697-732.
356

FIGURE CAPTIONS

Figure 1. Geographic location of the study area (**A**) and tectonic map of the Northwestern Alps (**B**) (modified after Balestro et al., 2015).

Figure 2. Geological map (**A**) and cross section (**B**) of the LMO. Photographs showing: the panoramic view of the unconformable contact (dotted blue line) of the Calcschist Unit (CSU) above the Composite Chaotic Complex (CCU) (**C**); D2 isoclinal folds deforming S1 foliation (defined by the serpentinite metarenite/calcschist contact) (**D**); D3 gentle folds ondulating the S2 foliation (**E**). Stratigraphic columns (**F**) and their three-dimensional correlation (**G**), showing the relationships between the ophiolite basement and the different types of chaotic rock units within the CCU.

Figure 3. View of the LMO and CCU: (**A**) Close up view of the meta-ophicalcite horizon consisting of serpentinite crosscutted by sets of veins, cm-thick, of carbonate, antigorite, or talc; (**B**) BrFm1 consisting of alternating clast- to matrix-supported ultramafic metabreccia horizons, followed by the BrFm3; (**C**) Close-up view of the BrFm2, showing disrupted and boudinated horizons of ultramafic metasandstone (arrows) embedded in a sheared carbonate-rich matrix to form the block-in-matrix arrangement; (**D**) Block-in-matrix fabric of the SedMé with dm- to meters wide “exotic” blocks of serpentinite (dashed white line), randomly distributed within a whitish marble matrix; (**E**) Close-up view of isolated blocks of ophicalcite with carbonate veins (arrows), decimeters long and 1-2 cm thick, in the SedMé. Note that veins are bounded within the blocks and do not cross the hosting whitish marble matrix; (**F**) Close-up view of the SedMé consisting of horizons of ultramafic metabreccia with angular clasts of serpentinite embedded within the marble matrix. (**G**) Close-up view of foliated (S2; dashed black line) ultramafic metabreccia in SedMé showing centimeter-sized, irregularly shaped clasts which mark the relict S1 foliation (dashed white line) deformed by D2 folds; (**H**) Disrupted horizons and bed fragments of ultramafic composition (arrows) embedded

384 within a matrix of alternating calcschist and marble beds of BrFm3; (**I**) Unconformable contact
385 (dotted line) of the Calcschist Unit above the serpentinite.
386
387 **Figure 4.** Cartoon showing different stages (**A-D**) of syn- to post-extensional intra-oceanic tectono-
388 sedimentary evolution of the CCU in Late Jurassic – Early Cretaceous time, and interpreted three-
389 dimensional intra-oceanic reconstruction of the physiography of the studied sector of the Ligurian-
390 Piedmont Ocean in Late Jurassic time (**E**) (inspired and modified from Escartin and Canales,
391 2011).
392

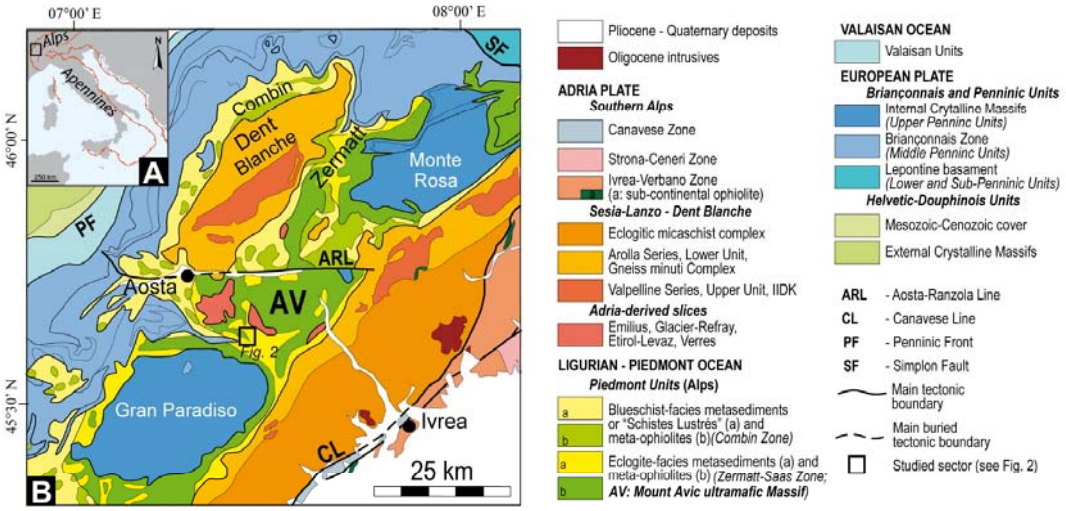

Fig 1 - *Tartarotti et al.*

393

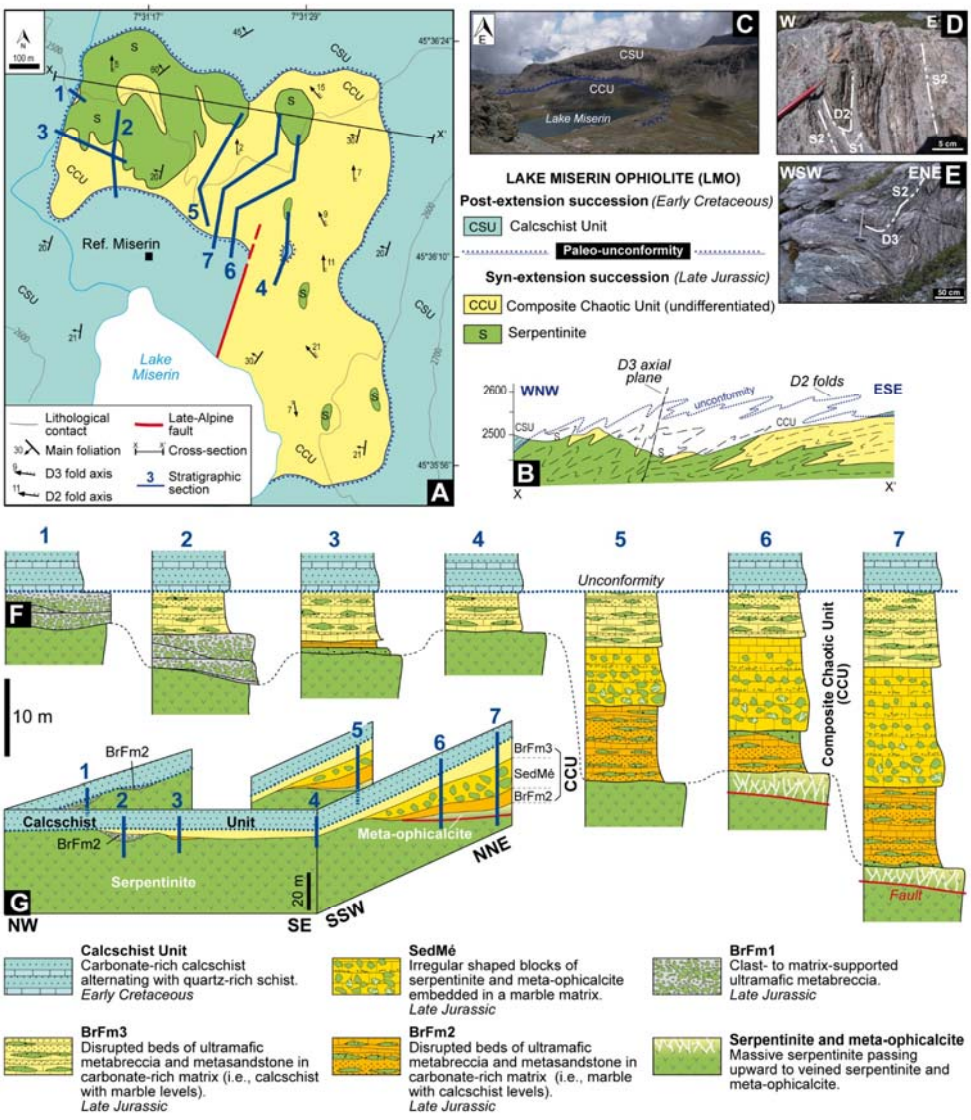

Fig 2 - *Tartarotti et al.*

394

395

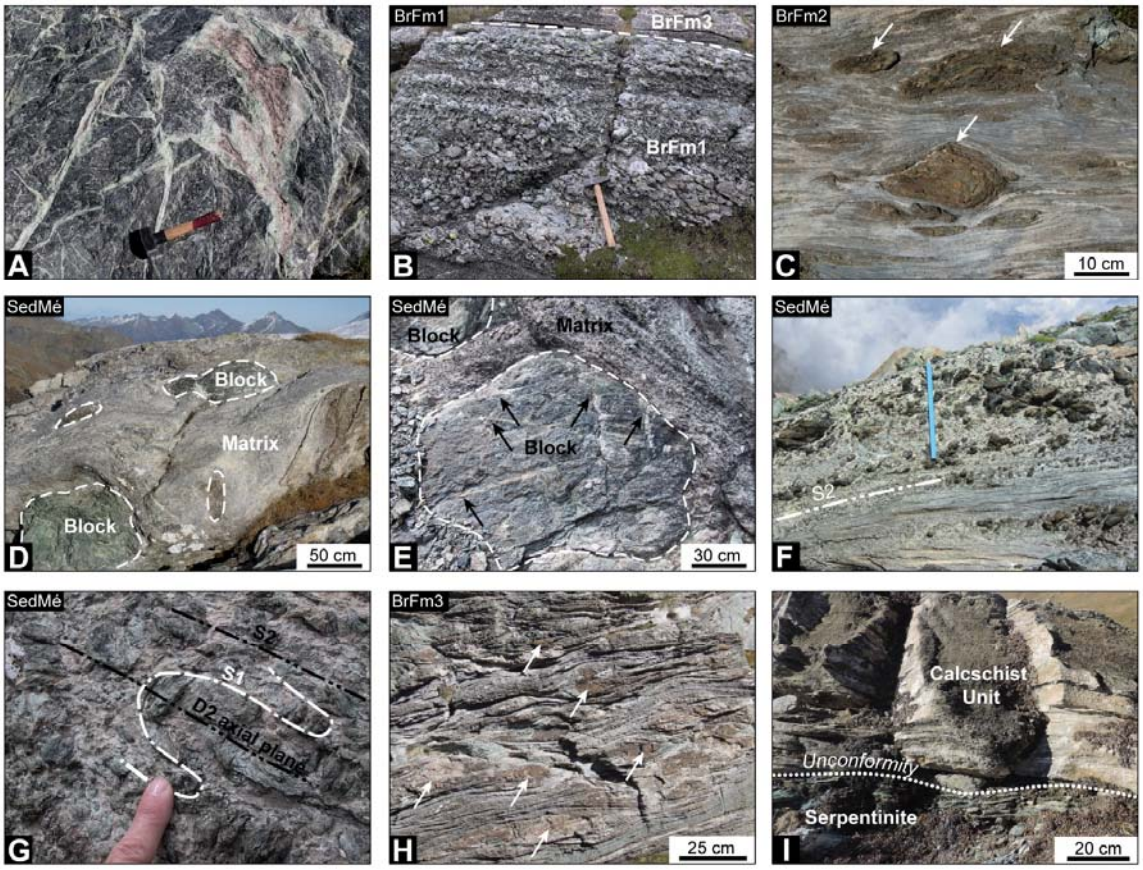

Fig. 3 - Tartarotti et al.

396

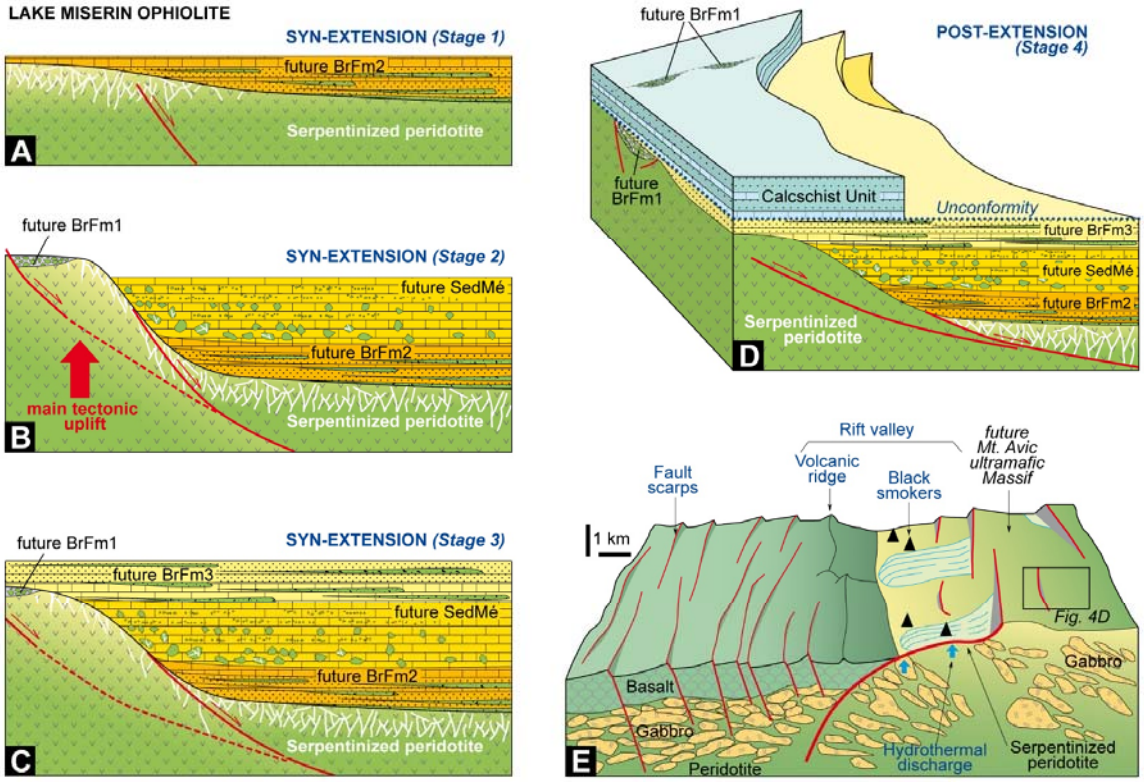

Fig. 4 - *Tartarotti et al.*

397